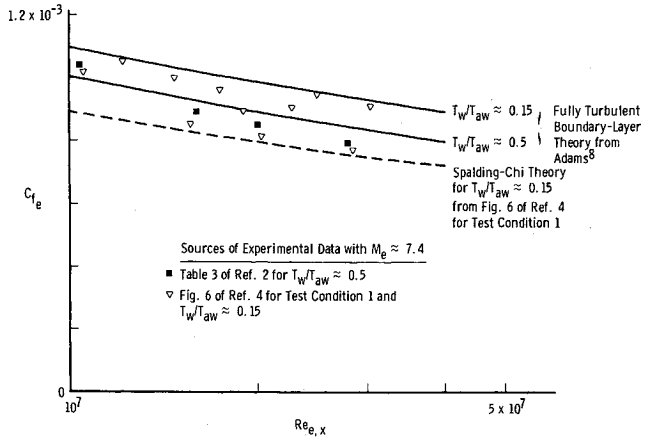

Fig. 3 Effects of wall temperature on skin friction for $M_e = 7.4$.

friction data of Ref. 4 based on application of a modified version of the Patankar-Spalding analysis.[12]

The important point from the above results is that analytical calculation techniques are indeed currently available which can yield valid and accurate values for sharp flat plate transitional and turbulent skin friction over a range of wall temperature ratios under hypersonic conditions, based on numerical integration of the governing boundary-layer equations using an eddy-viscosity model of turbulence and an intermittency factor treatment of transition. Through this approach one is not faced with the question of which semiempirical theory evaluated at what reference temperature is most appropriate for the flow under examination; exactly the same basic analysis is used for all flows.

References

[1] "Space Transportation System Technology Symposium. I-Aerothermodynamics and Configurations," TM X-52876, Vol. I, July 1970, NASA.

[2] Hopkins, E. J., Keener, E. R., and Dwyer, H. A., "Turbulent Skin Friction and Boundary-Layer Profiles Measured on Nonadiabatic Flat Plates at Hypersonic Mach Numbers," AIAA Paper 71-167, New York, 1971.

[3] Cebeci, T., "Calculation of Compressible Turbulent Boundary Layers with Heat and Mass Transfer," *AIAA Journal*, Vol. 9, No. 6, June 1971, pp. 1091–1097.

[4] Wallace, J. E., "Hypersonic Turbulent Boundary-Layer Studies at Cold Wall Conditions," *Proceedings of the 1967 Heat Transfer and Fluid Mechanics Institute*, Stanford University Press, 1967, pp. 427–451.

[5] Pearce, B. E., "A Comparison of Four Simple Calculation Methods for the Compressible Turbulent Boundary Layer on a Flat Plate," *Journal of Spacecraft and Rockets*, Vol. 7, No. 10, Oct. 1970, pp. 1276–1278.

[6] Neal, L., Jr., "A Study of the Pressure, Heat Transfer, and Skin Friction on Sharp and Blunt Flat Plates at Mach 6.8," TN D-3312, April 1966, NASA.

[7] Hopkins, E. J. and Inouye, M., "An Evaluation of Theories for Predicting Turbulent Skin Friction and Heat Transfer on Flat Plates at Supersonic and Hypersonic Mach Numbers," *AIAA Journal*, Vol. 9, No. 6, June 1971, pp. 993–1003.

[8] Adams, J. C., Jr., "Eddy Viscosity-Intermittency Factor Approach to Numerical Calculation of Transitional Heating on Sharp Cones in Hypersonic Flow," TR-70-210 (AD714058), Nov. 1970, Arnold Engineering Development Center, Arnold Air Force Station, Tenn.

[9] Harris, J. E., "Numerical Solution of the Equations for Compressible Laminar, Transitional, and Turbulent Boundary Layers and Comparisons with Experimental Data," TR R-368, Aug. 1971, NASA.

[10] Masaki, M. and Yakura, J., "Transitional Boundary Layer Considerations for the Heating Analysis of Lifting Re-Entry Vehicles," *Journal of Spacecraft and Rockets*, Vol. 6, No. 9, Sept. 1969, pp. 1048–1053.

[11] Mayne, A. W., Jr., and Dyer, D. F., "Comparisons of Theory and Experiment for Turbulent Boundary Layers on Simple Shapes at Hypersonic Conditions," *Proceedings of the 1970 Heat Transfer and Fluid Mechanics Institute*, Stanford University Press, 1970, pp. 168–188.

[12] Patankar, S. V. and Spalding, D. B., *Heat and Mass Transfer in Boundary Layers*, CRC Press, Cleveland, Ohio, 1968.

Structural Averaging of Stresses in the Hybrid Stress Model

JOHN P. WOLF*
Digital Ltd., Zurich, Switzerland

IN the finite-element method using the assumed stress hybrid model,[1,2] the statical behavior of the structural system is governed by the stress-displacement relations [Eq. (1)] and the equilibrium equations [Eq. (2)]

$$H \cdot \beta - T \cdot A^t \cdot u = -\delta o_\beta \tag{1}$$

$$A \cdot T^t \cdot \beta = P \tag{2}$$

where β = (unknown) stress-coefficient vector of all elements, u = (unknown) displacement vector of the nodal points, H = flexibility matrix of all elements, T^t = generalized concentrated force matrix of all elements, A = incidence matrix, δo_β = initial strain vector of all elements, and P = load vector of the nodal points (either applied directly or by premultiplying the "built-in" stress distribution, which has been integrated with the assumed boundary deformation, with the A matrix). In the H and T matrices, the corresponding matrices of the individual elements are assembled on the diagonal. For the sake of simplicity, in Eq. (1) it is assumed that no boundary deformations other than zero are prescribed. Reaction forces and the corresponding zero deformations have been eliminated from Eqs. (1) and (2).

Solving Eqs. (1) and (2), normally on an element basis, the u's and the β's are calculated. The stress distribution is determined from β, adding that of each element regarded as "built-in".[2] The stress field will, in general, exhibit finite discontinuities at the boundaries of each element. To calculate stresses at a nodal point, normally some kind of weighted average of stresses of the neighboring elements is determined. Many averaging procedures used in practice are based on arithmetic or geometrical but not on structural considerations. A review of present methods and a consistent procedure for displacement models are given in Ref. 3.

To average stresses structurally and thus to avoid discontinuities in certain points, additional equilibrium and/or continuity equations are added to Eq. (2) and indirectly also to Eq. (1). These express [Eq. (4b)] that the (final) stresses in certain interelement boundary points, normally where stress results are to be determined, are equal. They are a function of the β's. The modified stress-displacement [Eq. (3)] and equilibrium equations [Eqs. (4a) and (4b)] are

$$H \cdot \beta - T \cdot A^t \cdot u - t \cdot a^t \cdot q = -\delta o_\beta \tag{3}$$

$$A \cdot T^t \cdot \beta = P \tag{4a}$$

$$a \cdot t^t \cdot \beta = p \tag{4b}$$

t^t and a are the coefficient and incidence matrices, respectively. p, the right-hand side of the additional equations, is equal to the sum of the prescribed value (normally zero) and the negative "built-in" values of the neighboring elements, premultiplied by a, q is the vector of the corresponding additional deformations.

To avoid any kinematical deformation modes, the total number of stress modes (length of vector β) must be at least as large as the number of generalized displacements (sum of the lengths of the vectors u and q) after eliminating the rigid-body degrees of freedom of the structure. Care has to be taken to ensure that Eqs. (4a) and (4b) are linearly independent. By choosing the additional equations [Eq. (4b)] in such a way that together with Eq. (4a) the stresses across interelement boundaries are in equilibrium, an equilibrium model is derived. An analogous procedure of formulating additional equilibrium equations can be used to enforce systematically stress-boundary conditions.[4]

Solving Eq. (3) for β and substituting into Eqs. (4a) and (4b), we obtain

$$\beta = H^{-1} \cdot T \cdot A^t \cdot u + H^{-1} \cdot t \cdot a^t \cdot q - H^{-1} \cdot \delta o_\beta \tag{5}$$

Received December 22, 1971.

* Civil Engineer, Structural Department.

$$A \cdot T^t \cdot H^{-1} \cdot T \cdot A^t \cdot u + A \cdot T^t \cdot H^{-1} \cdot t \cdot a^t \cdot q = P + A \cdot T^t \cdot H^{-1} \cdot \delta o_\beta \quad (6a)$$

$$a \cdot t^t \cdot H^{-1} \cdot T \cdot A^t \cdot u + a \cdot t^t \cdot H^{-1} \cdot t \cdot a^t \cdot q = p + a \cdot t^t \cdot H^{-1} \cdot \delta o_\beta \quad (6b)$$

Eqs. (6a) and (6b) can be solved for u and q. β follows from Eq. (5). The (band) coefficient matrices and the right-hand sides of Eqs. (5) and (6) can be calculated on an element basis. For example, the stiffness matrix consisting of the submatrices $T^t \cdot H^{-1} \cdot T$, $T^t \cdot H^{-1} \cdot t$, $t^t \cdot H^{-1} \cdot T$ and $t^t \cdot H^{-1} \cdot t$ is assembled into the final system of equations with the total incidence matrix made up of A and a. This procedure, which makes use of "higher-order elements," leads to a larger system of equations (6) than if Eqs. (1) and (2) are processed (standard method); besides averaging stresses structurally in certain points, the over-all accuracy is improved.

The method can also be applied to a finite-element analysis using equilibrium models, if kinematical deformation modes can be avoided. The additional equations express that at least in certain points the stresses are continuous across interelement boundaries.

An approximation which splits the coefficient matrix of Eq. (6) into two submatrices, one of which $A \cdot T^t \cdot H^{-1} \cdot T \cdot A^t$ is the same as in the standard procedure, by which no additional equations are formulated [follows from Eqs. (1) and (2)], neglects the second coefficient matrix in Eq. (6a). Solving the modified Eq. (6a) for u and Eq. (6b) for q, we obtain

$$u = (A \cdot T^t \cdot H^{-1} \cdot T \cdot A^t)^{-1} \cdot (P + A \cdot T^t \cdot H^{-1} \cdot \delta o_\beta) \quad (7)$$

$$q = (a \cdot t^t \cdot H^{-1} \cdot t \cdot a^t)^{-1} \cdot (-a \cdot t^t \cdot H^{-1} \cdot T \cdot A^t \cdot u + p + a \cdot t^t \cdot H^{-1} \cdot \delta o_\beta) \quad (8)$$

β follows from Eq. (5). Starting from the displacements u determined by the standard procedure [Eq. (7)], a stress distribution β is calculated which satisfies the additional equilibrium and/or continuity equations. In general, all elements contribute to the (band) coefficient matrix

$$a \cdot t^t \cdot H^{-1} \cdot t \cdot a^t$$

of Eq. (8).

Applying the approximate procedure successively and individually to each point where stresses are to be averaged structurally, no coupling of the "additional stiffness matrix" $a \cdot t^t \cdot H^{-1} \cdot t \cdot a^t$ arises. If, for instance, the stresses are to be determined in nodal point 5 of the plate loaded in its plane (Fig. 1), a total of 9 additional equilibrium and continuity equations (3 each for n_x, n_y, n_{xy}) can be formulated in point 5. No additional equations are introduced in other points. The β distribution depends only on the u's in nodal points 1–9 [substituting Eq. (8) into Eq. (5)], thus on the same deformations as in the standard procedure. From a computational point of view, it may be advantageous to eliminate as many β's as there are additional equations using Eq. (4b) and q using some of the Eq. (3) (Ref. 4). Substituting into the remaining Eq. (3) and into Eq. (4a) shows that only the (four) H and T submatrices of the elements incident on the nodal point are affected (analogous for the right-hand sides). The method was developed while testing a large structural program system called STRIP (Ref. 5, p. 95).

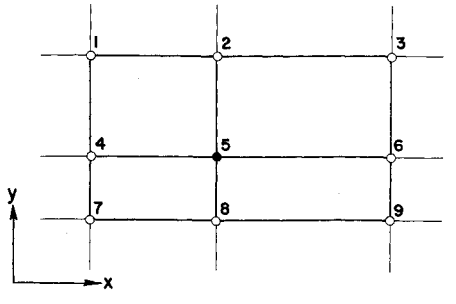

Fig. 1 Region of plate necessary for approximate structural averaging of stresses in point 5.

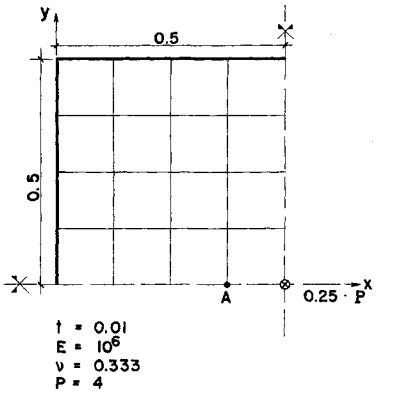

Fig. 2 Quarter of simply supported plate.

Numerical Example

A quarter of a simply supported square plate under a concentrated load is analysed with a 4×4 mesh (see Fig. 2). Assumed stress hybrid elements with a quadratic moment distribution over an element and a cubic displacement and linear rotation along the boundary are used. Stress-boundary conditions are not enforced, with the exception of the 24×24 mesh used for comparison. The approximate procedure [Eqs. (7) and (8)] is applied individually to point A. The stresses in this point are averaged structurally in two different ways: first, three equilibrium (m_x, m_{xy}, $m_{xy} = 0$) and one continuity (m_y) relations are used as additional equations, and second, five equilibrium (m_x, m_{xy}, q_x, $m_{xy} = 0$, $q_y = 0$) and two continuity relations (m_y, q_y) are formulated. That is, the continuity relation m_y expresses that the m_y at the corners at point A of the two elements are the same, the equilibrium relation m_x analogously for the m_x; the equilibrium equation $m_{xy} = 0$ formulated at the corner of any one of the two elements expresses that point A lies on an axis of symmetry.

The results are given in Table 1. In the first case, q_x and q_y are discontinuous; the arithmetic average is specified in the table. The results for the same 4×4 and a fine 24×24 mesh using the standard procedure [Eqs. (1) and (2)] are also given; the discontinuous values have been averaged arithmetically. It follows from the results that for this example, in general, the structural averaging process improves the accuracy. Only for m_y is the result of both structural averaging procedures less accurate than that using the standard method.

For comparison m_y is calculated using another averaging technique which is based on the equivalence of the stresses along the boundaries of the elements and the generalized concentrated nodal forces, which can be determined conveniently using the stiffness matrix $T^t \cdot H^{-1} \cdot T$ (Ref. 6). To determine m_y in point A, the section $y = 0$ is used. In Fig. 3, the concentrated forces (moments) of the two neighboring elements using the standard procedure are given. In point A, the values of the nodal forces in the corner of the two elements have been added. The simplest way of calculating m_y is to divide the concentrated nodal moment at A by the width of the element (0.09390/0.125 = 0.7512). An alternate method consists of assuming either a linear or a quadratic distribution of m_y along the boundary of the two neighboring elements (see Fig. 3). The moments expressed as a function of the 3 unknowns $m_y l$, $m_y o$, and $m_y r$ are integrated with the assumed boundary rotations (linear functions) cor-

Table 1 Comparison of results obtained by standard procedure and by approximate structural averaging

	24×24	4×4	4×4 Structural averaging	4×4 Structural averaging
	Standard procedure	Standard procedure	$m_x m_y m_{xy}$	$m_x m_y m_{xy}$ $q_x q_y$
m_x	−0.5247	−0.4475	−0.4838	−0.5793
m_y	−0.7206	−0.7064	−0.7505	−0.7719
m_{xy}	0.0000	−0.0113	0.0000	0.0000
q_x	−5.0627	−7.2091	−6.5254	−6.8214
q_y	0.0000	0.8158	1.2289	0.0000

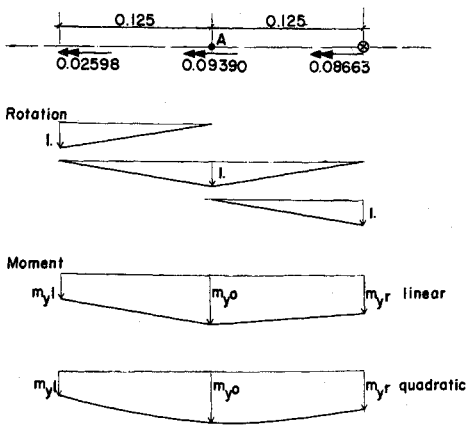

Fig. 3 Assumed distribution of rotation and of moment, equivalenced to concentrated nodal forces (moments) shown at top.

responding to the concentrated moments. Setting the integrals equal to the concentrated moments leads to a system of three equations. For the linear and quadratic assumptions of m_y, one can calculate $m_y o$, which is the value at A, as 0.6015 and 0.6764, respectively. It follows that all 3 values determined by using the nodal forces are less accurate than the approximate structural averaging procedure avoiding any discontinuities of the moments in point A (see Table 1). In both approaches only information from the neighboring elements is used.

References

[1] Pian, T. H. H., "Derivation of Element Stiffness Matrices by Assumed Stress Distributions," *AIAA Journal*, Vol. 2, No. 7, July 1964, pp. 1333–1336.

[2] Pian, T. H. H. and Tong, P., "Basis of Finite Element Methods for Solid Continua," *International Journal for Numerical Methods in Engineering*, Vol. 1, 1969, pp. 3–28.

[3] Oden, J. T. and Brauchli, H. J., "On the calculation of consistent stress distributions in finite element approximations," *International Journal for Numerical Methods in Engineering*, Vol. 3, 1971, No. 3, pp. 317–325.

[4] Wolf, J. P., "Systematic enforcement of stress boundary conditions in the assumed stress hybrid model based on the deformation method," *Proceedings of the First International Conference on Structural Mechanics in Reactor Technology*, Berlin, Germany, Sept. 1971, Commission of the European Communities, Brussels, Belgium.

[5] Bengtsson, Å. and Wolf, J. P., STRIP (Structural Integrated Programs), *Step S User Manual*, Digital Ltd., Zurich, and Nordisk. ADB, Stockholm, Aug. 1969.

[6] Turner, M. J., Martin, H. C., and Weikel, R. C., "Further development and applications of the stiffness method," *Matrix Methods of Structural Analysis*, AGARD 72, 1964, pp. 203–266.

Measurements of Reynolds Analogy for a Hypersonic Turbulent Boundary Layer on a Nonadiabatic Flat Plate

EARL R. KEENER* AND THOMAS E. POLEK*
NASA Ames Research Center, Moffett Field, Calif.

Nomenclature

C_f = local skin friction coefficient, τ_w/q_e
C_h = local Stanton number, $\dot{q}_w/\rho_e V_e(H_{aw}-H_w)$
H = enthalpy
M = Mach number
Pr = Prandtl number
q = dynamic pressure
$\dot{q}$ = heat-transfer rate
r = recovery factor
R_θ = Reynolds number based on boundary-layer momentum thickness
T = temperature
V = velocity
α = angle of attack of test surface to freestream
ρ = density
τ = shear stress

Subscripts
aw = adiabatic wall
e = boundary-layer edge
t = total
w = wall conditions

Received January 17, 1972.
* Research Scientist, Member AIAA.

A COMMON procedure for predicting aerodynamic heating of a surface immersed in a turbulent boundary layer is to use a method for predicting skin friction, together with a Reynolds analogy factor that relates heat transfer to skin friction. In a summary of available information on Reynolds analogy factors for zero-pressure-gradient boundary layers, Cary[1] points out that the often used value of $2C_h/C_f = 1.16$ (recommended in a study by Chi and Spalding) provides a good representation of experimental data for $M \lesssim 5$ and $T_w \approx T_{aw}$. However, for $M \gtrsim 5$, where considerable aerodynamic heating normally occurs, Cary concludes that there are insufficient data and too much scatter in existing data to empirically define the Reynolds analogy factor. Consequently, there is a need for accurate simultaneous measurements of skin friction and heat transfer at hypersonic Mach numbers, especially with conditions of considerable heat transfer.

Seven of the data points included by Cary[1] were preliminary measurements made on a flat plate at Ames and reported by Hopkins et al.[2] Simultaneous measurements of skin friction and heat transfer were made at $T_w/T_{aw} = 0.32$ and $R_\theta = 2600$ to 6200. Not all available data were published and additional measurements were later obtained at higher Reynolds numbers (R_θ up to 18,000). Reynolds analogy factors determined from these additional data from the flat plate test are presented herein.

The experimental investigation was conducted in air in the Ames 3.5 (ft Hypersonic Wind Tunnel, in which cold air is passed through an alumina storage heater system and heated to total temperatures ranging from about 670° to 1170°K. The nozzle was contoured to produce a flow at Mach 7.4. The model was a sharp-edged flat plate, 119 cm long by 43.8 cm wide, mounted on an injection mechanism outside the test section. Thin-skin heat-transfer gages were installed along the centerline of the thick-walled steel plate at 3.18 cm intervals. A skin-friction balance and a boundary-layer Pitot-pressure rake were mounted at 5.1 cm on each side of the centerline at a longitudinal station 100 cm from the leading edge. Measurement of τ_w and $\dot{q}_w$ are estimated to be accurate within 5%. The model was injected into the airstream at angles of attack of 9.3°, 6.2°, 3.1°, 0°, and −2.1°, resulting in Mach numbers at the boundary-layer edge of 5.9, 6.4, 6.9, 7.4 and 7.8, respectively. At each angle of attack the

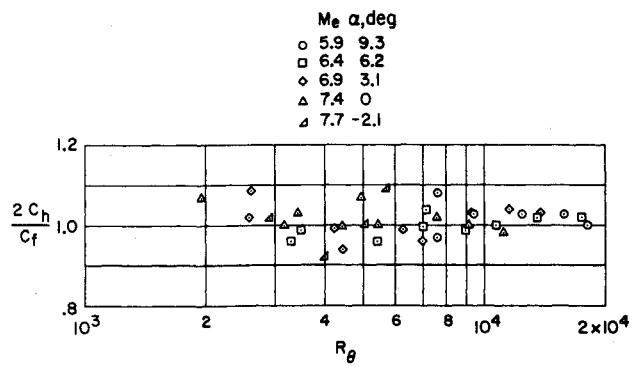

Fig. 1 Flat plate Reynolds analogy factor; T_w/T_{aw} = 0.3–0.5.